Assessing inherent and human-induced drivers of soil organic carbon to inform restoration activities in Rwanda

Leigh Ann Winowiecki[1], Aida Bargués-Tobella[2], Athanase Mukuralinda[3], Providence Mujawamaria[3], Elisée Bahati Ntawuhiganayo[3], Alex Mugayi[4], Susan Chomba[1], Tor-Gunnar Vågen[1]

[1]World Agroforestry (ICRAF), Nairobi, Kenya
[2] Department of Forest Ecology and Management, Swedish University of Agricultural Sciences (SLU), Umeå, Sweden
[3] World Agroforestry (ICRAF), Kigali, Rwanda
[4] World Vision- Rwanda
Correspondence to: Leigh Ann Winowiecki (L.A.Winowiecki@cgiar.org)

Abstract

Land degradation negatively impacts water, food and nutrition security and is leading to increased competition for resources. While landscape restoration has the opportunity to restore ecosystem function, understanding the drivers of degradation is critical for prioritizing and tracking interventions. We sampled 300-1000m^2 plots using the Land Degradation Surveillance Framework across Nyagatare and Kayonza districts in Rwanda to assess key soil and land health indicators, including soil organic carbon (SOC), erosion prevalence, vegetation structure and infiltration capacity and their interactions. SOC content decreased with increasing sand content across both sites and sampling depths and was lowest in croplands and grasslands compared to shrublands and woodlands. Stable carbon isotope values (δ^{13}C) ranged from -15.35 to -21.34 ‰ indicating a wide range of plant communities with both C3 and C4 photosynthetic pathways. Field-saturated hydraulic conductivity (K_{fs}) was modeled, with a median of 76 mm h^{-1} in Kayonza and 62 mm h^{-1} in Nyagatare, respectively. Topsoil OC had a positive effect on Kfs, whereas pH, sand and erosion had negative effects. Soil erosion was highest in plots classified as woodland and shrubland. Maps of soil erosion and SOC at 30-m resolution were produced with high accuracy and showed high variability across the region. These data demonstrate the inherent and anthropogenic controls of SOC, and the additive impact on critical ecosystem functions and services, including soil hydrological functioning. By understanding these relationships we can better prioritize interventions that result in multiple benefits, as well as assess the impact of restoration options.

1. Introduction

Land degradation is inextricably linked to livelihoods and negatively impacts over 3.2 billion people each year globally (IPBES, 2018). Land degradation also adversely affects the resilience of social-ecological systems to climate change by reducing their adaptive capacity. Therefore, the combined impacts of land degradation and climate change represent a significant risk to global food security (Webb et al., 2017), particularly when considering positive feedback effects between processes such as more erratic and intense rainfall events and soil erosion. Similarly, land degradation strongly impacts the loss of biodiversity globally, further reducing the adaptive capacity of ecosystems in the face of climate change (Gisladottir and Stocking, 2005), which means that we cannot tackle any of these global challenges in isolation.

Efforts to avoid, reduce and reverse land degradation are therefore critical if the Sustainable Development Goals (SDGs) are to be achieved (IPBES, 2018). SDG 15.3, Life of Land has set ambitious targets for land degradation neutrality (LDN), combining belowground indicators, i.e., soil organic carbon (SOC), and aboveground measures (net primary productivity and land use) (Cowie et al., 2018). In line with this thinking, forest and landscape restoration aims to regain ecological functions, including biodiversity and soil function, and enhance human well-being across landscapes (Chazdon, 2008; Chazdon et al., 2016). The UN Decade on Ecosystem Restoration (2021-2030) offers promising opportunities to bring together the global community to scale efforts across the globe. However, ecosystems are complex and multiple biophysical and socio-economic factors need to be considered when targeting, planning, implementing and tracking restoration on the ground. This includes understanding the spatial and biogeochemical variations of the soil ecosystem, which is the foundation for biophysical land restoration efforts given its role in global net primary productivity.

The global community acknowledges the need for long-term monitoring networks across diverse environments (Navarro et al., 2017; Sachs et al., 2010), including those focused on soil monitoring (Guerra et al., 2021; Lehmann et al., 2020; Vermeulen et al., 2019), in order to better understand drivers and interactions as well as track progress of interventions. However, many assessments of land degradation and restoration suffer from (i) disagreements about the definition of land degradation, (ii) a conundrum of indicators that are often not feasible to measure and hence operationalize, and (iii) a lack of rigorous science-based analytical frameworks (Vågen, 2015). Indicators are critical when assessing ecosystem health and tracking progress toward restoration targets or climate actions, and can be important communication tools for decision makers. Indicators should be readily measurable, quantifiable and encompass the complexity of various drivers. The call for soil degradation and resilience indicators is not new (Lal, 1997), however, scientific research around the concept of soil health continues (Lehmann et al., 2020). Despite this, SOC is widely accepted as a key indicator of soil health, due to its influence on multiple indicators and its response to aboveground processes, including land management (Deb et al., 2015; Paustian et al., 2019; Shikuku et al., 2017). In addition, SOC is seen as a key indicator to monitor progress on a number of SDGs (Lorenz et al., 2019).

Accelerated soil erosion is arguably the most important indicator of land degradation and also one of the most widespread forms of degradation worldwide (Bennett, 1939; Lal, 2003; Pimentel, 2006; Vågen and Winowiecki, 2019). Given the heterogeneity of landscapes, spatial information on the distribution of these indicators needs to be made at relevant spatial scales (i.e. at the farm, landscape, and regional levels). Furthermore, interactions between these indicators need to be considered explicitly. Recent advancements in spatially explicit assessment of soil and land health that combine field-based campaigns with data analytics and earth observation are now paving the way for improved methods of biophysical characterization of multiple indicators (Vågen et al., 2016) while providing an opportunity to enable science-based monitoring approaches that can be applied in restoration prioritization (Winowiecki et al., 2018) as well as for communication with decision makers (Vågen et al., 2018a).

In Rwanda, land degradation continues to be a critical challenge. To combat this, Rwanda set a goal to achieve land degradation neutrality by 2030 and, in 2011, Rwanda was the first country in Africa to commit to a restoration target of degraded lands and forests under the Bonn Challenge, pledging to restore 2 million ha, corresponding to 76% of the country. Underlying causes of land degradation in the country include unsustainable farming and grazing practices, overexploitation of forests and woodlands, settlements and urbanization (Bizimana, 2018). One of the major processes of land degradation in Rwanda is accelerated soil erosion, which is driven by unsustainable agricultural practices, particularly in steeply sloping lands (Karamage et al., 2016). This is further exacerbated by intense rainfall events, resulting in increased rainfall erosivity (Rutebuka et al., 2020) and the increasing energy demands of a growing population resulting in deforestation and loss of vegetation cover in general (Mukuralinda et al., 2016). Soil erosion is severe with mean national rates of 250 Mg ha^{-1} yr^{-1}, and studies showing as much as 421 Mg ha^{-1} yr^{-1} in croplands (Karamage et al., 2016).

Considering that the agricultural sector contributes significantly to the national economy and that 90% of the population depends on agriculture for their livelihoods, tackling land degradation and restoring degraded land is of critical importance for Rwanda. Studies suggest that investments in soil conversation and land productivity are contributing to reduced land degradation and increased agricultural productivity in Rwanda (Bidogeza et al., 2015; Byiringiro and Reardon, 1996; Fleskens, 2007; Bizoza and De Graaff, 2012; Karamage et al., 2016). For example, various forms of terracing have been implemented across Rwanda to specifically curb the negative effects of intensive farming on steep slopes on soil fertility and soil loss (Kagabo et al., 2013). Studies also show that terracing coupled with building organic matter has the potential to be financially profitable when access to labour and manure is facilitated (Bizoza and de Graaff, 2012). Furthermore, there is a real need for a systems approach to sustainable agricultural intensification that spans from appropriate technologies to institutional and policy-level support (Schut et al., 2016; Vanlauwe et al., 2014). In addition, agroforestry approaches have also been suggested to meet the multiple demands of farming households, including in Rwanda (Liyama et al., 2018).

In this paper, we applied a systematic approach to collecting data on soil health and land degradation indicators, including the use of soil spectroscopy, using the Land Degradation Surveillance Framework (LDSF) (Vågen and Winowiecki, 2020) across agricultural-dominated landscapes in eastern Rwanda. Specific objectives of this study were to: 1) Assess soil and land health indicators across two landscapes; 2) Understand the drivers of SOC dynamics; 3) Develop hot-spot maps of soil erosion and soil organic carbon for restoration interventions. We assessed the relationship between inherent soil properties such as texture and SOC, as well as the influence of various soil properties on field-saturated hydraulic conductivity, in addition to human-induced processes such as soil erosion. We also assess the current status of vegetation structures across the landscape, including tree densities and tree species diversity. We present spatially-explicit assessments and maps of SOC for eastern Rwanda and explore key inherent and human-induced drivers of SOC across landscapes in the eastern part of the country.

2. Methods

2.1. Site Description

The LDSF was conducted in two districts in eastern Rwanda, Nyagatare and Kayonza. Nyagatare is the largest dairy district in Rwanda and is characterised by two main seasons: one long dry season and a short rainy season. Its annual average temperature varies between 25.3 and 27.7 °C, and it receives an annual rainfall of 827 mm, however rainfall patterns have become increasingly unpredictable and variable. The average altitude is 1,513m. It consists of gently sloping hills separated by low granitic valleys. The vegetation type was originally savannah vegetation and some gallery forests. From 2009 to 2019, there was a net loss of forest cover with deforestation and afforestation rates at 34% and 18%, respectively (MoE, 2019). The major economic activity is subsistence farming while the main source of cooking energy is fuel wood. Multiple crops are cultivated in Nyagatare including, maize, beans, groundnut, cassava, irish potatoes, banana, and yams, among others. Some areas have been cultivated for 100 years, but the majority of the agricultural expansion in the district took place between 1973 and 1995. The dominant soil types in Nyagatare wereFerralsols (Oxisols) with shallow Leptosols on hillsides, according to data from the Ministry of Agriculture (MINAGRI).

Kayonza district has a mean altitude of 1,428 m and a mean annual rainfall of 919 mm (NISR, 2012). It is prone to long drought events with two principal seasons, a long dry period and a short rainy season. . Crops cultivated in Kayonza include beans, banana, cassava, maize, irish potato, sorghum, cocoa yams, among others. Most of the area has been cultivated for over 50 years, with mining activities also taking place. Dominant soil types in the Kayonza site were Ferralsols and Leptosols, with Histosols in lower-lying areas.

2.2. Field Sampling using the Land Degradation Surveillance Framework

The LDSF was developed by the World Agroforestry (ICRAF) in response to the need for a consistent field method and indicator framework to assess soil and land health at the landscape-scale. The framework has been applied in several projects across the global tropics (Vågen et al., 2016; Vågen and Winowiecki, 2020, 2019) and is currently one of the largest ecosystem health databases globally, with data from more than 30,000 plots in over 40 countries. The LDSF uses a hierarchical sampling design to simultaneously measure and assess several land and soil health indicators. An LDSF site is a 100 km^2 area stratified into 16-1 km^2 clusters, each containing 10-1000 m^2 plots and 4-100 m^2 subplots (L.

Winowiecki et al., 2016). The hierarchical sampling design enables robust analysis of drivers of degradation as well as the production of predictive maps of soil health indicators, for example soil organic carbon (Vågen et al., 2018b). The two LDSF sites in this study were randomized within each of the districts. The field team navigated to the randomized plots and set up the four circular subplots within the plot.

Measurements took place at the plot and subplot levels. All plots were geo-referenced to better than 5m accuracy. Vegetation structure was classified at the plot level using the FAO Land Cover Classification System (LCCS), which was developed in the context of the FAO-AFRICOVER project (Di Gregorio, A., and Jansen, 2000). Specifically, plots were classified as either annual cropland, grassland, shrubland, woodland or forest vegetation structure. In the LDSF, trees are classified as woody vegetation above 3 m tall, whereas woody plants 1.5-3 m height are classified as shrubs. All trees were counted and identified to species level in each of the four subplots per plot. Soil erosion was scored and classified in each subplot (n=4) per plot. Specifically, each subplot was visibly assessed for erosion (i.e., rill, sheet or gully), otherwise the plot was marked as having no erosion. Erosion scores (presence (1) or absence (0)) were used in the statistical analysis. Soil samples were collected using a soil auger at the center of each subplot at two depths (0-20 cm (topsoil) and 20-50 cm (subsoil)). Soil samples were combined from the four subplots into one composite sample per LDSF plot and depth increment.

Infiltration capacity was measured at three plots per cluster in each site using single ring infiltrometers (Bouwer, 1986) to assess variation across land uses and soil types. Soil infiltration capacity into dry soils follows a predictable temporal pattern: it is high in the early stages of infiltration and tends to decline gradually as the soil moisture content increases until it eventually approaches a nearly constant rate known as steady-state infiltration capacity (Horton, 1940). This steady-state rate is independent of the initial soil water content and approximates the soil's saturated hydraulic conductivity. Infiltration measurements were carried out at the center of each plot using a metal cylinder with an inner diameter of 15.6 cm and 20 cm in height for two hours and a half to ensure capturing steady-state conditions.

Field-saturated hydraulic conductivity (Kfs) (Reynolds and Elrick, 1990) was calculated from the infiltration data using the analytical formula proposed by Nimmo et al. (2009). First, infiltration rates were corrected for non-constant falling head and subsurface lateral spreading effects. For each plot, an asymptotic function was then fitted to its corrected infiltration curve using the *nls.multstart* package in R (Padfield and Matheson, 2018) to obtain the asymptote, which represents Kfs.

The effects of soil and land use and land cover variables on Kfs were assessed with linear mixed effects models using the *lme4* package (Bates et al., 2015) in R. Random effects intercept models were fitted using the lmer function, with random intercept for each level of site and for each level of cluster within site (nested grouping factors). To assess statistical significance of fixed effects, we used the *lmerTest* package in R (Kuznetsova et al., 2017).

2.3. Laboratory Methods

Upon collection, all soil samples were processed locally in Rwanda, air-dried and ground to pass through a 2-mm sieve. Air-dried and ground samples were packed and shipped to the ICRAF Soil-Plant Spectral Diagnostics Laboratory in Nairobi, Kenya. Further grinding was then conducted on a subsample using a Retsch motor grinder to attain a particle size between 20 and 53 microns. This subsample was analyzed in triplicate for MIR absorbance using a Tensor 27 HTS-XT from Bruker Optics in the ICRAF Soil-Plant Spectral Diagnostics Laboratory in Nairobi, Kenya. The measured wavebands ranged from 4000 to 601 cm^{-1} with a resolution of 4 cm^{-1}. Processing of the MIR spectra included computing the first derivatives using a Savitsky-Golay polynomial smoothing filter implemented in the locpoly function of the *KernSmooth* R package (Wand, 2015) as outlined in Terhoeven-urselmans et al., (2010).

Wet chemistry reference analysis was conducted on 10% of the collected soil samples (n=32 samples per site, 16 topsoil and 16 subsoil samples). Soil pH and exchangeable bases were measured at Crop Nutrition Laboratory Services in Nairobi, Kenya. Soil pH was analyzed in a 1:2 H_2O mixture that was shaken for 30 min at moderate speed on a horizontal shaker then let stand for 20 min before reading on a Eutech Cyberscan 1100 pH meter. Exchangeable bases were extracted using the Mehlich-3 method after five minutes on a reciprocating shaker. The filtrate was analyzed for base cations: potassium (K), calcium (Ca), magnesium (Mg) and sodium (Na) using an ICP OES (Model-Thermo iCAP6000 Series). Total nitrogen, organic carbon and stable carbon isotopes ($\delta^{13}C$) were measured by dry combustion using an Elemental Analyzer Isotope Ratio Mass Spectrometry (EA-IRMS) from Europa Scientific after removing inorganic C with 0.1 N HCl, at the IsoAnalytical Laboratory located in the United Kingdom. Stable carbon isotopes were expressed as $\delta^{13}C$ in parts per mile (‰) relative to the V-PDB (Pee Dee Belemnite) standard. Sand content was measured using a Laser Diffraction Particle Size Analyzer (LDPSA) from HORIBA (LA 950) after shaking each soil sample for four minutes in a 1% sodium hexametaphosphate (calgon) solution, at the World Agroforestry Centre (ICRAF) Soil-Plant Spectral Diagnostics Laboratory in Nairobi, Kenya.

2.4. Prediction of soil properties from MIR soil spectroscopy

Soil samples with both MIR spectra and associated wet chemistry data were used to train (calibrate) predictive models in order to simultaneously predict multiple soil properties using random forest (RF) regression models (Vågen et al., 2016). In the RF algorithm, many decision trees are built, each on a bootstrap sample, based on a random subset of the input MIR spectra and these trees are combined to predict the different soil properties. The total number of reference samples used for model development and testing were 10,820 for SOC, 7,305 for soil pH, 4,322 for soil texture and 1,657 for $\delta^{13}C$. In training the prediction models, we randomly selected 70% of the samples for each soil property, keeping the remaining 30% out for testing of the models. We then calculated R^2 and Root Mean Square Error of Prediction (RMSEP) values for the training and test dataset to assess model performance.

2.5. Landscape level mapping of soil erosion and SOC

We used LDSF soil and field data from a total of 30,853 sites in 40 countries, including the two sites from this study, to generate prediction models and map SOC and soil erosion based on Landsat 8 reflectance data. The approach we followed in this study is described in Vågen et al. (2013), but we applied Landsat 8 rather than Landsat 7 and a larger database of LDSF sites. A Landsat 8 spectral library was built for all of the LDSF plots by extracting surface reflectance values for each band, matching remote sensing data acquisition to within six months of field survey dates. Cloud masking was conducted prior to surface reflectance extraction. We then used the annual median reflectance values for each band as input into the prediction models for SOC and erosion in order to map SOC concentrations (gC kg^{-1}) and the probability of erosion (in %) for each 30m Landsat pixel.

We assessed the performance of the prediction models in a similar manner as for the soil MIR predictions, by using 70% of the plots to train the models and the remaining 30% to test performance. For erosion, we assessed model performance by calculating the percentage of correctly classified test instances relative to observed instances, expressed as a confusion matrix and by calculating the Receiver Operating Characteristic curve (ROC) (Bradley, 1997), which evaluates the accuracy of a model by considering errors that are either *false positives* or *false negatives*.

3. Results

3.1. Vegetation structure and diversity in the LDSF plots sampled

LDSF field surveys took place between October and November 2018. In total, 151 plots were sampled in Kayonza and 149 plots were sampled in Nyagatare. Both sites were dominated by annual cropping systems, with 68% of the sampled plots in Kayonza classified as cultivated and 89% in Nyagatare. Other vegetation structure classes included shrubland (19% in Kayonza, 3.4% in Nyagatare), woodland (9.3% in Kayonza and 7.4% in Nyagatare) and grassland (3.3% in Kayonza). Mean tree density was higher in Nyagatare (120 tree ha^{-1}) compared to Kayonza (68 tree ha^{-1}). Overall this level of tree density is low, and the higher tree densities only occurred in woodlots of *Eucalyptus spp.* (Figure 1). Mean tree density in croplands were 57 tree ha^{-1} in Kayonza and 35 tree ha^{-1} in Nyagatare. The plots with higher tree density in croplands were dominated by *Eucalyptus spp*. In total 62 unique tree species were identified in the two LDSF sites. The most common species was: *Eucalyptus spp*., followed by *Grevillea robusta*, *Euphorbia tirucalli*, *Ricinus communis*, *Mangifera indica*, *Carica papaya* and *Senna spectabillis* (Figure 2). Differences were observed between the two LDSF sites, most notably that *Jatropha curcas* was only found in Kayonza and *Senna singueana* was only found in Nyagatare. (Figure 2). In summary, 48 unique species were observed in Kayonza and 39 species in Nyagatare. This level of tree diversity is considered quite low, with a low occurrence of most species and low occurrence of only a few indigenous species, and a dominance of *Eucalyptus spp*. For example, 171 (56%) of the sampled plots had *Eucalyptus spp.*, including 125 of the cropland plots (53%).

3.2. MIR prediction results for soil properties

Prediction performance was good for the soil properties included in the study, including for the prediction of $\delta^{13}C$, as summarised in Table 1. The prediction model performance for $\delta^{13}C$ is similar to that reported by (Winowiecki et al., 2017) when predicting $\delta^{13}C$ based on near-infrared (NIR) spectroscopy. Figure 3 shows predicted versus measured SOC and $\delta^{13}C$, respectively, for Nyagatare and Kayonza, showing good model performance across a wide range of SOC and $\delta^{13}C$, respectively.

3.3. Soil properties and erosion prevalence

Soil properties for top and sub soil samples for Kayonza (n= 151, 136) and Nyagatare (n= 149, 145) LDSF sites are presented in Table 2. Density plots for the soil variables demonstrate the variability between and within the sites (Figure 3). Overall, pH values were low across the two sites, with statististical differences in topsoil pH values between sites ($P<0.001$), mean topsoil pH in Kayonza was 5.65 and 5.89 in Nyagatare . This level of pH can potentially limit agricultural production. Both sites had low overall exchangeable bases (Ca, K, Mg, Na), as 8 cmol$_c$ kg^{-1} is considered critically low for agricultural productivity. Kayonza had significantly higher clay content and lower sand content compared to Nyagatare ($P<0.001$). Kayonza had statistically higher topsoil OC content (20.9 g kg^{-1}) compared to Nyagatare (17.3 g kg-^{1}) ($P<0.001$). Figure 5 shows the relationship between sand content and SOC content, with SOC increasing with decreased sand content for both sites and both depths (Figure 4). This demonstrates the important control of inherent soil properties, i.e., sand content, on SOC. The same pattern was observed in each vegetation structure. However, SOC was lowest in the cropland and grassland plots compared to shrublands and woodlands ($P<0.001$). Average $\delta^{13}C$ was -18.9 ‰ in Kayonza and -19.2 ‰, in Nyagatare, which indicates that these are mixed C3-C4 systems. We also assess the variation of stable carbon isotopes within and between the vegetation structure classes (Figure 6). While there are some distinctions between vegetation classes, namey more negeative isotope values in woodlands compared to croplands, the overlap is due to the high occurrence of *Eucalyptus spp*., even in cropland plots and that woodland plots were previously cultivated, resulting in the mixed C3-C4 signal.

Kayonza had higher soil erosion prevalence with 45% of the plots considered severely eroded, compared to 27% of the sampled plots in Nyagatare. The dominant erosion categories were rill and sheet. Severe erosion was more prevalent in woodland (91%), shrubland and grassland (77%), compared to cropland (25%). This is most likely given the high prevalence of terracing in the region as well as the location of the cropping fields compared to woodland and bushland. For example, the average slope for the plots classified as cultivated was seven degrees compared to 19 degrees for the other vegetation classes. There was no statistical difference in SOC in severely eroded and non-severely eroded plots, however cropland plots were the dominant category across the landscape and only 24% of cropland plots were classified as severely eroded.

3.4. Saturated hydraulic conductivity

Median topsoil field-saturated hydraulic conductivity (Kfs) in Kayonza was 76 mm h^{-1}, whereas in Nyagatare it was 62 mm h^{-1} (Figure 7). In Kayonza, Kfs was not only higher but also more variable than in Nyagatare, with an interquartile range (upper quartile – lower quartile) of 77 mm h^{-1} and 42 mm h^{-1}, respectively.

Results from the linear mixed effects (lme) models showed that the presence of erosion and pH had both a significant negative effect on Kfs ($P < 0.025$ and $P < 0.016$, respectively). Topsoil OC had a nearly significant ($P <0.082$) positive effect on Kfs, whereas sand content had a significant negative effect ($P <0.033$).We could not assess the effect of vegetation structure on Kfs, as most of the plots where infiltration was measured were on cropland.

3.5. Soil mapping

Soil erosion prevalence was predicted with a high degree of accuracy using Landsat 8 satellite data, with an out-of-bag prediction (OOB) error of 14%. The OOB prediction error-rate is based on a bootstrap sample of about 37% of unused test observations and represents a robust assessment of accuracy. Further to the calculation of the OOB error-rate, the receiver operator characteristics (ROC) curve also indicates good model performance with the area under the ROC curve (AUC) calculated at 0.86. These results are consistent with previous studies using remote sensing to predict erosion (Vågen et al., 2013; Vågen and Winowiecki, 2019). Given the level of accuracy, we applied the random forest model to Landsat 8 imagery for 2018, generating a map of soil erosion at 30-m resolution for the study area. Hotspots of erosion are shown in red and yellow in the map in Figure 8, representing areas where erosion prevalence is predicted to be over 60% in 2018, some areas also having extreme erosion (>75%). As we can see from this map, there is high spatial variability of erosion across eastern Rwanda.

The prediction model performance for SOC was also good, with an R^2 of 0.82 based on the OOB prediction results from the random forest model and testing of the prediction model on an independent test dataset (Figure 9). The map of SOC (Figure 10) shows high levels of variation in SOC across the study area with particularly low SOC in Nyagatare district, with the exception of wetlands along rivers and in forested areas in the west of the district. The map shows higher SOC in protected areas and in lower lying areas, including in wetlands in the eastern part of the study area.

4. Discussion

The LDSF was used to assess soil and land health indicators across two landscapes in eastern Rwanda. Both sites (Kayonza and Nyagatare). Both sites were dominated by annual cropping systems, and both sites had overall low tree densities and low tree diversity. *Eucaltypus spp* dominated both the woodland and cropland systems in both sites, followed by *Grevillea robusta*. *Jatropha curcas* was observed only in Kayonza and *Senna singueana* was only observed in Kayonza. These data have important implications for restoration activities. For example tree planting is in the global spotlight as a restoration activity that has high potential for climate change mitigation, while providing multiple other ecosystem services (Bastin et al., 2019). However, the global community acknowledges that tree planting and reforestation must do down taking into account multiple environmental and socio-economic considerations. For example, prioritize appropriate areas to restore, use of natural regeneration, maximize biodiversity, among other principles (Di Sacco et al., 2021). In Rwanda, there are multiple tree planting campaigns funded by the government as well as within the development sector. These data demonstrate a real opportunity to improve tree biodiversity across the landscape, including on cultivated fields. While woodlands reportedly had higher SOC content compared to the other vegetation structure classes, woodlands also had mixed land use history, from native vegetation, to being cultivated, leading to the high variation in SOC values. These findings of low diversity are similar to those of other studies from other regions of Rwanda (Bucagu et al., 2013; Liyama et al., 2018), highlighting the opportunity for the strategic inclusion of useful and appropriate tree species that fulfill multiple ecosystem benefits, including the inclusion of indigenous tree species on farm.

This paper highlights the importance of assessing key soil and land health indicators, most notably SOC and soil erosion. The concept of soil health goes beyond individual indicators, and is more about building and maintaining a functioning soil ecosystem to provide and support multiple ecosystem services and functions. Lehman et al., (2020) discussed the shift of focus of soil assessments from crop productivity to human health, climate change adaptation and mitigation and water quality and quantity. This shift acknowledges the linkages across multiple indicators, and this information can be used to prioritize interventions to maximize benefits and minimize tradeoffs.

For example, inherent soil properties, such as soil texture, is influenced by parent material, and while sand content is not sensitive to management, it does limit the ability of the soil to store or sequester carbon. In Figure 5, we show the relationship between sand content and SOC in the two LDSF sites included in the study. The trend of decreasing SOC with increasing sand content in these data is well established and has been reported in other studies using the LDSF from Tanzania (Winowiecki et al., 2016). This relationship is related to factors such as surface area of soil mineral particles, which decreases with increasing sand content leaving less area that SOC can be absorbed onto. Acknowledging this influence on SOC and other key properties is important for understanding restoration potential in terms of soil health as well as climate change mitigation potential.

The boxplots in Figure 6 show both predicted $\delta^{13}C$ and SOC across vegetation structure classes in the two LDSF sites. Generally, we see the lowest SOC contents and also higher $\delta^{13}C$ values in cropland, indicating SOC derived from C4 vegetation such as maize (*Zea mais*). In areas where SOC is derived from vegetation with a C3 photosynthetic pathway, such as woodlands and shrublands we also have higher SOC values. These results showed lowest SOC in croplands, despite wide variation, which indicates and opportunity to increase SOC through management practices. This is especially apparent when assessing the effect of soil erosion on SOC. Soil erosion prevalence was more prominent in woodland, shrubland and grassland LDSF plots in the two sites, compared to cropland plots. Indicating that farmers are already managing for erosion, which is an essential first step in building soil health, including maintaining and building SOC. Seventy-six percent of cropland plots were scored as not having severe erosion, with 24% having severe erosion. While SOC variation in both categories (severely eroded and not severely eroded, there was now statistical difference in SOc content, which differs from other studies that found erosion to have a strong effect of SOC content and stocks (Vågen and Winowiecki, 2013; Leigh Winowiecki et al., 2016). Both Nyagatare and Kayonza sites had low overall soil pH and exchangeable bases. However, these data are in line with what Vågen et al. (2016) reported using data from 114 LDSF sites across sub-Saharan Africa (SSA), e.g., their results showed an overall mean of topsoil OC of 22 g kg-1, a mean pH value of 6.1 and mean sum of bases of 15 $cmol_c kg^{-1}$.Since very few plots were sampled under naturally vegetated, undisturbed, sites, our analysis is limited in terms of extending this into semi-natural systems. This was also reflected in the C3-C4 signal in the $\delta^{13}C$ data, which mostly reflected mixed C3-C4 systems.

This highlights the need to use multiple indicators to understand drivers of SOC dynamics, including interactions between plant communities, management, and inherent soil properties.

Field-saturated hydraulic conductivity (Kfs) is highly variable in the two study sites, as shown in Figure 7, with Nyagatare having slightly lower Kfs rates than Kayonza. SOC positively influenced Kfs, which is in agreement with previous findings highlighting the importance of soil organic matter for soil aggregation and water infiltration (Franzluebbers, 2002).Our results indicate that sand content influences Kfs negatively, which is counterintuitive, as coarse-textured soils tend to have higher Kfs compared to more fine-grained soils (Hillel, 1980; García Gutiérrez et al. 2017). However, soil hydraulic properties of soils with finer textures have been shown to be less dependent on particle size distribution (García Gutiérrez et al. 2017), which could partially explain our results considering that sand content in the plots where infiltration was measured was relatively low. It is also likely that the negative relationship between sand content and Kfs we have found reflects the positive effect of SOC on Kfs, as SOC and sand content had a strong negative relationship. On the other hand, soil pH and the presence of erosion had a negative effect on Kfs. Erosion and land degradation often lead to reduced soil infiltration capacity due to a decline in SOC and subsequent deterioration of soil structure (Valentin & Bresson,1997), which in turn can result in increased infiltration-excess overland flow and further erosion (Blake et al., 2018). Our findings indicate the complexity in determining hydrologic controls across landscapes, which is something that will need to be studied in more detail in the future. Maintaining and promoting soil hydrological functioning is critical for food and water security and to build resilience to climate change (Bossio et al., 2010) (Bossio et al., 2009, Falkenmark & Rockström 2008, Cole et al. 2008), but this is often overlooked in the discussions around restoration. Findings from this study highlight the importance of human-induced drivers on Kfs and, therefore, the potential to actively maintain and restore soil hydrological functioning.

By applying a consistent indicator framework such as the LDSF, which combines systematic field measurements with innovative laboratory methods, advanced data analytics and remote sensing, we are able to conduct spatial assessments of SOC, erosion and other land health indicators with high levels of accuracy. Such assessments and maps have applications not only for targeting of land restoration interventions, but also for tracking of changes overtime. For example, by mapping SOC at 30-m resolution, we can pick up spatial patterns related to both land management and inherent soil properties to identify both drivers of land degradation and land restoration potential, including SOC sequestration.

In a case study from the Lake Kivu area of Rwanda (Akayezu et al., 2020) showed the utility of erosion hotspot mapping for spatial targeting of soil and water conservation measures. The results of the study presented here can be used in a similar manner to identify hotspots (Figure 8) within the study area where erosion is occurring. These hotspots can in turn be combined with spatial assessments of SOC (Figure 10) to more effectively target areas for land restoration, particularly where there is high erosion prevalence and low SOC. This is critically important, particularly if we consider the often high economic costs of restoring degraded land (Quillérou and Thomas, 2012) and the importance of land restoration for achieving the Sustainable Development Goals (Herrick et al., 2019). Furthermore, by combining spatially explicit indicators of land and soil health spatial prioritization of restoration potential based on biophysical characteristics can enable decision making (Winowiecki et al., 2018)

5. Conclusions

We demonstrate the utility of systematic, multi-scale assessments of soil and land health across landscapes to target and monitor ecosystem restoration interventions, including the importance of understanding the interactions between indicators. By using a robust set of soil and land health indicators that are consistently sampled and characterized, we are able to provide analysis and spatial assessments at scales relevant to smallholder farmers across. In the current study we illustrate the approach with examples for SOC and erosion, although additional indicators may be included to address the complexity of land degradation and tailor land restoration interventions that consider interactions of multiple indicators in a spatially explicit way. We also demonstrate the importance of understanding both inherent and human-induced drivers of indicators such as SOC, which is critical for landscape restoration. We highlight the link between SOC, erosion, and hydrologic function. Using these data, we suggest land managers implement restoration options that reduce erosion, increase soil organic carbon and increase aboveground biodiversity. Doing so have the potential to reach multiple goals, includie food and nutrition security, climate change mitigation and adaption and biodiversity. We argue that there is an urgent need for systematic assessments of SOC, as well as aboveground biodiversity (e.g., tree diversity), combined with hydrologic properties and other indicators of land degradation such as soil erosion to effectively target interventions across landscapes. This will not only ensure that appropriate interventions for land restoration are implemented, but also provide the evidence base to assess their effectiveness.

Rwanda is one of the most progressive countries in the region in terms of acknowledging the importance of landscape restoration for sustainable livelihoods. It has set ambitious targets over the next decade, aiming to restore more than 76% of its land area. Given the importance of the agricultural sector in the country and widespread land degradation due to a combination of deforestation and unsustainable agricultural practices, there is a need for evidence to support the targeting of land restoration efforts, as well as for tracking of the effectiveness of such interventions over time. By combining systematic field based surveys with advances in soil spectroscopy and earth observation data, we can model and map SOC concentrations with high accuracy, allowing us to identify areas for restoration and track interventions over time.

6. Data Availability

All LDSF data are posted here:
https://data.worldagroforestry.org/dataverse/icraf_soils

7. Sample Availability

All soil samples are logged and barcoded at the ICRAF Soil-Plant Spectral Diagnostics Laboratory at World Agroforestry (ICRAF) in Nairobi, Kenya.

8. Team List

See acknowledgements and author list.

9. Author Contribution

LW and TGV co-led the conceptualization, writing and analysis. AM and AlexM led the coordination of the field work and contributed to the writing. PM contributed to collection of field data and interpretation. EBN and AlexM contributed to interpretation of the results. SC contributed to the contextualization. ATB contributed to the analysis, in particular to the infiltration analysis and modeling as well as the writing. LW prepared the manuscript with contributions from all co-authors.

10. Competing Interest

"The authors declare that they have no conflict of interest."

11. Disclaimer

The views expressed in this paper do not necessarily reflect the views of the donors who funded thisi work.

11.1. Special Issue Statement

This article is part of the Special Issue: *Tropical Biogeochemistry of soils in the Congo Basin and the African Great Lakes region.*

11.2. Acknowledgements

The authors would like to thank the partners who participated in the LDSF field surveys, including World Vision-Rwanda staff including: Jeremie Harerima, Donatien Niyibigira, Patrick Rugema, Thomas Habanabakize, Lambert Bucyana, Gilberrt Abakundanye, Augustin Tuyiturriki. Rwanda Agriculture Body, including Lambert Musengimana, Thomas Gakwavu, and Mukobwa Bijou, as well as Minani Vedaste from the Forestry Centre and John Thiongo Maina. We also acknowledge the staff of the ICRAF Soil-Plant Diagnostic Laboratory for the logging and organizing the soil samples as well as analysis of MIR Spectra. These project activities were supported through the funding of the European Union within the project dubbed, "Regreening Africa", grant number DCI-ENV/2017/387-627. We also acknowledge funding from the Swedish Research council Formas, grant number 2017-00430. Finally this research was funded in part by the CGIAR Research Programme (CRP) Forests, Trees and Agroforestry (FTA) and the CGIAR Research Programme (CRP) on Water, Land and Ecosystems .

12. References

Akayezu, P., Musinguzi, L., Natugonza, V., Ogutu-Ohwayo, R., Mwathe, K., Dutton, C., Manyifika, M., 2020. Using sediment fingerprinting to identify erosion hotspots in a sub-catchment of Lake Kivu, Rwanda. Environ. Monit. Assess. 12.

Bastin, J., Finegold, Y., Garcia, C., Mollicone, D., Rezende, M., Routh, D., Zohner, C.M., Crowther, T., 2019. The global tree restoration potential. Science (80-.). 79, 76–79.

Bates, D., Maechler, M., Bolker, B., Walker, S., 2015. Fitting Linear Mixed-Effects Models Using lme4. J. Stat. Softw. 67, 1–48. https://doi.org/doi:10.18637/jss.v067.i01

Bennett, H.H., 1939. Soil changes due to erosion, in: Soil Science Society Proceedings. pp. 399–401.

Bidogeza, J., Berentsen, P., De Graaff, J., Oude Lansink, A., 2015. Bio-economic modelling of the influence of family planning, land consolidation and soil erosion on farm production and food security in Rwanda. J. Dev. Agric. Econ. 7, 204–221. https://doi.org/10.5897/jdae2013.0481

Bizimana, I., 2018. Final Country Report of the LDN Target Setting ProgrammeinRwanda. Kigali.

Bizoza, A.R., de Graaff, J., 2012. Financial cost-benefit analysis of bench terraces in Rwanda. L. Degrad. Dev. 23, 103–115. https://doi.org/10.1002/ldr.1051

Blake, W.H., Rabinovich, A., Wynants, M., Kelly, C., Nasseri, M., 2018. Soil erosion in East Africa : an interdisciplinary approach to realising pastoral land management change Soil erosion in East Africa : an interdisciplinary approach to realising pastoral land management change.

Bossio, D., Geheb, K., Critchley, W., 2010. Managing water by managing land: Addressing land degradation to improve water productivity and rural livelihoods. Agric. Water Manag. 97, 536–542.

Bouwer, H., 1986. Intake rate: cylinder infiltrometer, in: Klute, A. (Ed.), Methods of Soil Analysis. Part 1. Physical and Mineralogical Methods. American Society of Agronomy, Madison, Wisconsin, pp. 825–844.

Bradley, A., 1997. The use of the area under the ROC curve in the evaluation of machine learning algorithms. Pattern Recognit. 30, 1145–1159.

Bucagu, C., Vanlauwe, B., Van Wijk, M.T., Giller, K.E., 2013. Assessing farmers' interest in agroforestry in two contrasting agro-ecological zones of Rwanda. Agrofor. Syst. 87, 141–158. https://doi.org/10.1007/s10457-012-9531-7

Byiringiro, F., Reardon, T., 1996. Farm productivity in Rwanda: effects of farm size, erosion, and soil conservation investments. Agric. Econ. 15, 127–136. https://doi.org/https://doi.org/10.1111/j.1574-0862.1996.tb00426.x

Chazdon, R.L., 2008. Beyond deforestation: Restoring forests and ecosystem services on degraded lands. Science (80-.). 320, 1458–1460. https://doi.org/10.1126/science.1155365

Chazdon, R.L., Brancalion, P.H.S., Lamb, D., Laestadius, L., Calmon, M., Kumar, C., 2016. A Policy-Driven Knowledge Agenda for Global Forest and Landscape Restoration. Conserv. Lett. https://doi.org/10.1111/conl.12220

Cowie, A.L., Orr, B.J., Castillo Sanchez, V.M., Chasek, P., Crossman, N.D., Erlewein, A., Louwagie, G., Maron, M., Metternicht, G.I., Minelli, S., Tengberg, A.E., Walter, S., Welton, S., 2018. Land in balance: The scientific conceptual framework for Land Degradation Neutrality. Environ. Sci. Policy 79, 25–35. https://doi.org/10.1016/j.envsci.2017.10.011

Deb, S., Bhadoria, P.B.S., Mandal, B., Rakshit, A., Singh, H.B., 2015. Soil organic carbon: Towards better soil health, productivity and climate change mitigation. Clim. Chang. Environ. Sustain. 3, 26. https://doi.org/10.5958/2320-642x.2015.00003.4

Di Gregorio, A., and Jansen, L.J.M., 2000. Land Cover Classification System (LCCS): Classification Concepts and User

Manual. Fao 53, 179. https://doi.org/10.1017/CBO9781107415324.004

Di Sacco, A., Hardwick, K.A., Blakesley, D., Brancalion, P.H.S., Breman, E., Cecilio Rebola, L., Chomba, S., Dixon, K., Elliott, S., Ruyonga, G., Shaw, K., Smith, P., Smith, R.J., Antonelli, A., 2021. Ten golden rules for reforestation to optimize carbon sequestration, biodiversity recovery and livelihood benefits. Glob. Chang. Biol. 1–21. https://doi.org/10.1111/gcb.15498

Franzluebbers, A., 2002. Soil organic matter stratification ratio as an indicator of soil quality. Soil Tillage Res.

Gisladottir, G., Stocking, M., 2005. Land degradation control and its global environmental benefits. L. Degrad. Dev. 16, 99–112. https://doi.org/https://doi.org/10.1002/ldr.687

Guerra, B.C.A., Bardgett, R.D., Caon, L., Crowther, T.W., Montanarella, L., Navarro, L.M., Orgiazzi, A., Singh, B.K., Tedersoo, L., Vargas-rojas, R., Briones, M.J.I., Buscot, F., Cameron, E.K., Cesarz, S., Chatzinotas, A., Cowan, D.A., Djukic, I., Hoogen, J. Van Den, Maestre, F.T., Marín, C., Reitz, T., Rillig, M.C., Smith, L.C., Vries, F.T. De, Weigelt, A., Wall, D.H., Eisenhauer, N., 2021. Tracking, targeting, and conserving soil biodiversity. Science (80-.). 37, 239–242.

Herrick, J.E., Abrahamse, J.E., Abhilash, P.C., Ali, S.H., Alvarez-Torres, P., Barau, A.S., Branquinho, C., Chhatre, A., Chotte, J.L., Cowie, A.L., Davis, K.F., Edrisi, S.A., Fennessy, M.S., Fletcher, S., Flores-Díaz, A.C., Franco, I.B., Ganguli, A.C., Speranza, C.I., Kamar, M.J., Kaudia, A.A., Kimiti, D.W., Luz, A.C., Matos, P., Metternicht, G., Neff, J., Nunes, A., Olaniyi, A.O., Pinho, P., Primmer, E., Quandt, A., Sarkar, P., Scherr, S.J., Singh, A., Sudoi, V., von Maltitz, G.P., Wertz, L., Zeleke, G.A., 2019. Land Restoration for Achieving the Sustainable Development Goals - An International Resource Panel Think Piece. Nairobi, Kenya.

IPBES, 2018. The IPBES assessment report on land degradation and restoration, in: Montanarella, L., Scholes, R., Brainich, A. (Eds.), Secretariat of the Intergovernmental Science-Policy Platform on Biodiversity and Ecosystem Services. p. 744.

Kagabo, D.M., Stroosnijder, L., Visser, S.M., Moore, D., 2013. Soil erosion, soil fertility and crop yield on slow-forming terraces in the highlands of Buberuka, Rwanda. Soil Tillage Res. 128, 23–29. https://doi.org/https://doi.org/10.1016/j.still.2012.11.002

Karamage, F., Zhang, C., Ndayisaba, F., Shao, H., Kayiranga, A., Fang, X., Nahayo, L., Nyesheja, E.M., Tian, G., 2016. Extent of cropland and related soil erosion risk in Rwanda. Sustain. 8, 1–19. https://doi.org/10.3390/su8070609

Kuznetsova, A., Brockhoff, P.B., Christensen, R.H.B., 2017. lmerTest Package: Tests in Linear Mixed Effects Models . J. Stat. Softw. 82. https://doi.org/10.18637/jss.v082.i13

Lal, R., 2003. Soil erosion and the global carbon budget 29, 437–450. https://doi.org/10.1016/S0160-4120(02)00192-7

Lal, R., 1997. Degradation and resilience of soils. Philos. Trans. R. Soc. B Biol. Sci. 352, 997–1010. https://doi.org/10.1098/rstb.1997.0078

Lehmann, J., Bossio, D.A., Kögel-Knabner, I., Rillig, M.C., 2020. The concept and future prospects of soil health. Nat. Rev. Earth Environ. 1, 544–553. https://doi.org/10.1038/s43017-020-0080-8

Liyama, M., Mukuralinda, A., Ndayambaje, J.D., Musana, B., Ndoli, A., Mowo, J.G., Garrity, D., Ling, S., Ruganzu, V., 2018. Tree-Based Ecosystem Approaches (TBEAs) as multi-functional land management strategies-evidence from Rwanda. Sustain. 10. https://doi.org/10.3390/su10051360

Lorenz, K., Lal, R., Ehlers, K., 2019. Soil organic carbon stock as an indicator for monitoring land and soil degradation in relation to United Nations' Sustainable Development Goals. L. Degrad. Dev. 30, 824–838. https://doi.org/10.1002/ldr.3270

Navarro, L.M., Fernández, N., Guerra, C., Guralnick, R., Kissling, W.D., Londoño, M.C., Muller-Karger, F., Turak, E., Balvanera, P., Costello, M.J., Delavaud, A., El Serafy, G.Y., Ferrier, S., Geijzendorffer, I., Geller, G.N., Jetz, W., Kim, E.S., Kim, H.J., Martin, C.S., McGeoch, M.A., Mwampamba, T.H., Nel, J.L., Nicholson, E., Pettorelli, N., Schaepman, M.E., Skidmore, A., Sousa Pinto, I., Vergara, S., Vihervaara, P., Xu, H., Yahara, T., Gill, M., Pereira, H.M., 2017. Monitoring biodiversity change through effective global coordination. Curr. Opin. Environ. Sustain. 29, 158–169. https://doi.org/10.1016/j.cosust.2018.02.005

Nimmo, J.R., Schmidt, K.M., Perkins, K.S., Stock, J.D., 2009. Rapid Measurement of Field-Saturated Hydraulic Conductivity for Areal Characterization. Vadose Zo. J. 8, 142. https://doi.org/10.2136/vzj2007.0159

Padfield, D., Matheson, G., 2018. nls.multstart: Robust Non-Linear Regression using AIC Scores. R package version 1.0.0.

Paustian, K., Collier, S., Baldock, J., Burgess, R., Creque, J., Delonge, M., Dungait, J., Ellert, B., Frank, S., Goddard, T., Govaerts, B., Grundy, M., Henning, M., Izaurralde, R.C., Mcconkey, B., Porzig, E., Rice, C., Searle, R., Seavy, N., Skalsky, R., Mulhern, W., Jahn, M., Paustian, K., Collier, S., Baldock, J., Burgess, R., Creque, J., Delonge, M., Dungait, J., Ellert, B., Frank, S., Goddard, T., Govaerts, B., Henning, M., Izaurralde, R.C., Madaras, M., Mcconkey, B., Porzig, E., Rice, C., Searle, R., Seavy, N., Skalsky, R., Mulhern, W., Jahn, M., 2019. Quantifying carbon for agricultural soil management : from the current status toward a global soil information system. Carbon Manag. 0, 1–21. https://doi.org/10.1080/17583004.2019.1633231

Pimentel, D., 2006. Soil erosion: a food and environmental threat. Env. Dev Sustain 8, 119–137.

Quillérou, E., Thomas, R., 2012. Costs of land degradation and benefits of land restoration: A review of valuation methods and suggested frameworks for inclusion into policy-making (No. 0606). https://doi.org/10.1079/PAVSNNR20127060

Reynolds, W., Elrick, D., 1990. Ponded infiltration from a single ring: I. Analysis of steady flow. Soil Sci. Soc. Am. J. 54, 1233–1241.

Rutebuka, J., De Taeye, S., Kagabo, D., Verdoodt, A., 2020. Calibration and validation of rainfall erosivity estimators for application in Rwanda. CATENA 190, 104538. https://doi.org/https://doi.org/10.1016/j.catena.2020.104538

Sachs, J., Remans, R., Smukler, S., Winowiecki, L., Cassman, K., Castle, D., DeFries, R., Fanzo, J., Jackson, L.E., Leemans, R., Lehmann, J., Milder, J., Naeem, S., Nziguheba, G., Palm, C., Reganold, J., Tomich, T., Scherr, S., Sircely, J., Sullivan, C., Sanchez, P., 2010. Monitoring the world's agriculture. Nature 466, 11–13.

Schut, M., van Asten, P., Okafor, C., Hicintuka, C., Mapatano, S., Nabahungu, N.L., Kagabo, D., Muchunguzi, P., Njukwe, E., Dontsop-Nguezet, P.M., Sartas, M., Vanlauwe, B., 2016. Sustainable intensification of agricultural systems in the

Central African Highlands: The need for institutional innovation. Agric. Syst. 145, 165–176. https://doi.org/10.1016/j.agsy.2016.03.005

Shikuku, K.M., Valdivia, R.O., Paul, B.K., Mwongera, C., Winowiecki, L., Läderach, P., Herrero, M., Silvestri, S., 2017. Prioritizing climate-smart livestock technologies in rural Tanzania: A minimum data approach. Agric. Syst. 151. https://doi.org/10.1016/j.agsy.2016.06.004

Terhoeven-urselmans, T., Vagen, T., Spaargaren, O., Shepherd, K.D., 2010. Prediction of Soil Fertility Properties from a Globally Distributed Soil Mid-Infrared Spectral Library. Soil Sci. Soc. Am. J. 74. https://doi.org/10.2136/sssaj2009.0218

Vågen, T.-G., 2015. Methods for Assessing the Impacts of IFAD ASAP-supported Projects on Land and Ecosystem Degradation 12.

Vågen, T.-G., Winowiecki, L.A., 2020. Land Degradation Surveillance Framework (LDSF): Field Guide v2020. Nairobi, Kenya.

Vågen, T.-G., Winowiecki, L.A., 2013. Mapping of soil organic carbon stocks for spatially explicit assessments of climate change mitigation potential. Environ. Res. Lett. 8. https://doi.org/10.1088/1748-9326/8/1/015011

Vågen, T.-G., Winowiecki, L.A., Abegaz, A., Hadgu, K.M., 2013. Landsat-based approaches for mapping of land degradation prevalence and soil functional properties in Ethiopia. Remote Sens. Environ. 134, 266–275.

Vågen, T.-G., Winowiecki, L.A., Neely, C., Chesterman, S., Bourne, M., 2018a. Spatial assessments of soil organic carbon for stakeholder decision-making. A case study from Kenya. SOIL Discuss. 1–14. https://doi.org/10.5194/soil-2017-37

Vågen, T.-G., Winowiecki, L.A., Neely, C., Chesterman, S., Bourne, M., 2018b. Spatial assessments of soil organic carbon for stakeholder decision-making: A case study from Kenya. SOIL 4, 259–266. https://doi.org/10.5194/soil-2017-37

Vågen, T.-G., Winowiecki, L.A., Tondoh, J.E., Desta, L.T., Gumbricht, T., 2016. Mapping of soil properties and land degradation risk in Africa using MODIS reflectance. Geoderma 263, 216–225.

Vågen, Winowiecki, 2019. Predicting the Spatial Distribution and Severity of Soil Erosion in the Global Tropics using Satellite Remote Sensing. Remote Sens. 11, 1800. https://doi.org/10.3390/rs11151800

Vanlauwe, B., Coyne, D., Gockowski, J., Hauser, S., Huising, J., Masso, C., Nziguheba, G., Schut, M., Van Asten, P., 2014. Sustainable intensification and the African smallholder farmer. Curr. Opin. Environ. Sustain. 8, 15–22. https://doi.org/10.1016/j.cosust.2014.06.001

Vermeulen, S., Bossio, D., Lehmann, J., Luu, P., Paustian, K., Webb, C., Augé, F., Bacudo, I., Baedeker, T., Havemann, T., Jones, C., King, R., Reddy, M., 2019. A global agenda for collective action on soil. Nat. Sustain. 2, 2–4. https://doi.org/10.1038/s41893-018-0212-z

Wand, M., 2015. KernSmooth: Functions for Kernel Smoothing Supporting Wand & Jones (1995).

Webb, N.P., Marshall, N.A., Stringer, L.C., Reed, M.S., Chappell, A., Herrick, J.E., 2017. Land degradation and climate change: building climate resilience in agriculture. Front. Ecol. Environ. 15, 450–459. https://doi.org/10.1002/fee.1530

Winowiecki, Leigh, Vågen, T.-G., Huising, J., 2016. Effects of land cover on ecosystem services in Tanzania: A spatial assessment of soil organic carbon. Geoderma 263, 274–283. https://doi.org/10.1016/j.geoderma.2015.03.010

Winowiecki, L., Vågen, T.-G., Massawe, B., Jelinski, N.A., Lyamchai, C., Sayula, G., Msoka, E., 2016. Landscape-scale variability of soil health indicators: effects of cultivation on soil organic carbon in the Usambara Mountains of Tanzania. Nutr. Cycl. Agroecosystems 105. https://doi.org/10.1007/s10705-015-9750-1

Winowiecki, L.A., Vågen, T.-G., Boeckx, P., Dungait, J.A.J., 2017. Landscape-scale assessments of stable carbon isotopes in soil under diverse vegetation classes in East Africa: application of near-infrared spectroscopy. Plant Soil. https://doi.org/10.1007/s11104-017-3418-3

Winowiecki, L.A., Vågen, T.-G., Kinnaird, M.F., O'Brien, T.G., 2018. Application of systematic monitoring and mapping techniques: Assessing land restoration potential in semi-arid lands of Kenya. Geoderma 327. https://doi.org/10.1016/j.geoderma.2018.04.017

Table 1:Prediction model performance metrics for the prediction of soil properties from MIR spectroscopy included in the study.

Soil property	R^2		RMSEP	
	Training	Testing	Training	Testing
SOC	0.99	0.92	1.3	3.3
d13C	0.97	0.72	0.8	1.8
pH	0.97	0.84	0.2	0.4
Sum of exchangeable bases	0.96	0.84	3.9	8.2
Sand	0.98	0.84	3.1	8.9
Clay	0.98	0.82	3.5	10.1

Table 2: Soil properties for top and sub soil samples at the two LDSF sites (SD = standard deviation, ExBases is exchangeable bases) .

Site	Depth	N	Mean SOC	SD SOC	Mean d13C	SD dC13	Mean pH	SD pH	Mean ExBaes	SD ExBases	Mean Sand	SD Sand	Mean Clay	SD Clay
	cm		g kg^{-1}		‰				$cmol_c$ kg^{-1}			%		

Kayonza	0-20	151	20.9	8.83	-18.9	1.15	5.65	0.68	10.3	8.69	19.8	9.29	58.4	11.5
	20-50	136	16.9	7.96	-18.4	1.26	5.65	0.65	10.6	9.10	19.4	9.27	60.6	11.4
Nyagatare	0-20	149	17.3	6.07	-19.2	0.92	5.89	0.54	8.74	4.80	30.0	10.2	44.5	10.5
	20-50	145	13.3	5.49	-18.7	0.97	5.88	0.55	8.44	5.77	30.0	10.5	45.8	11.4

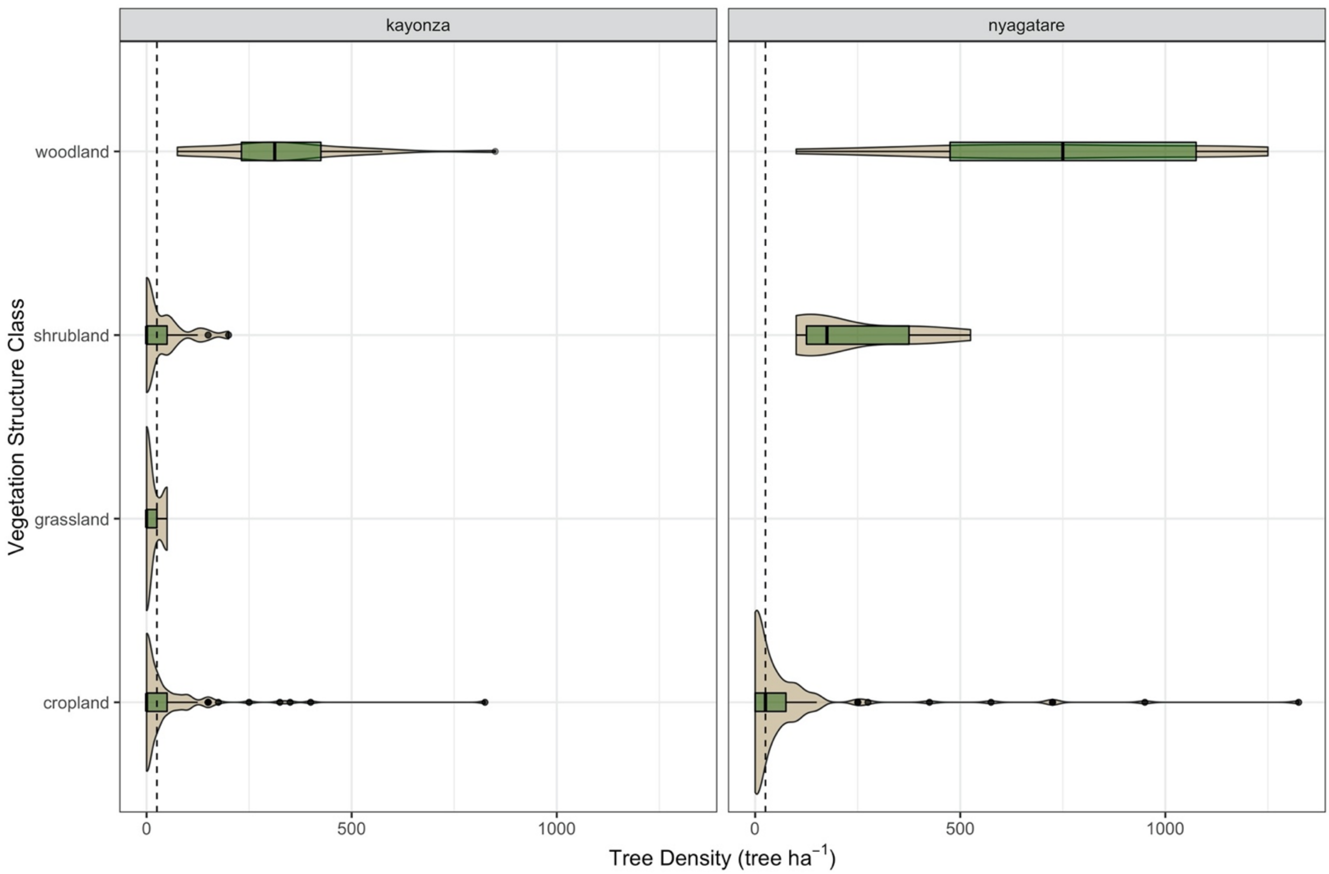

Figure 1: Violin plots showing the variation in tree densities across the vegetation classes at both LDSF sites. The dotted line is the overall median (25 tree ha^{-1}).

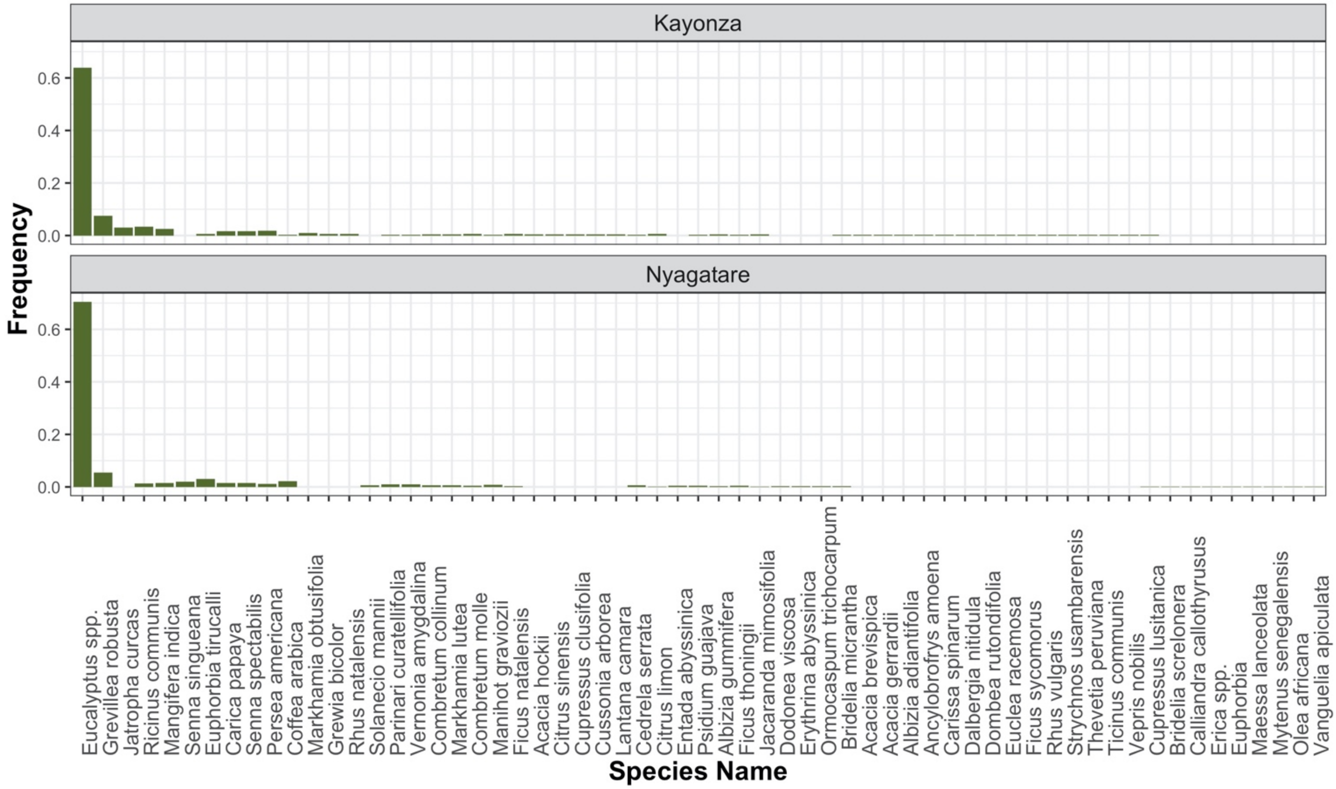

Figure 2: Tree species across the two LDSF sites. Sixty-two different species were recorded, with low occurrence of most species, and few indigenous tree species.

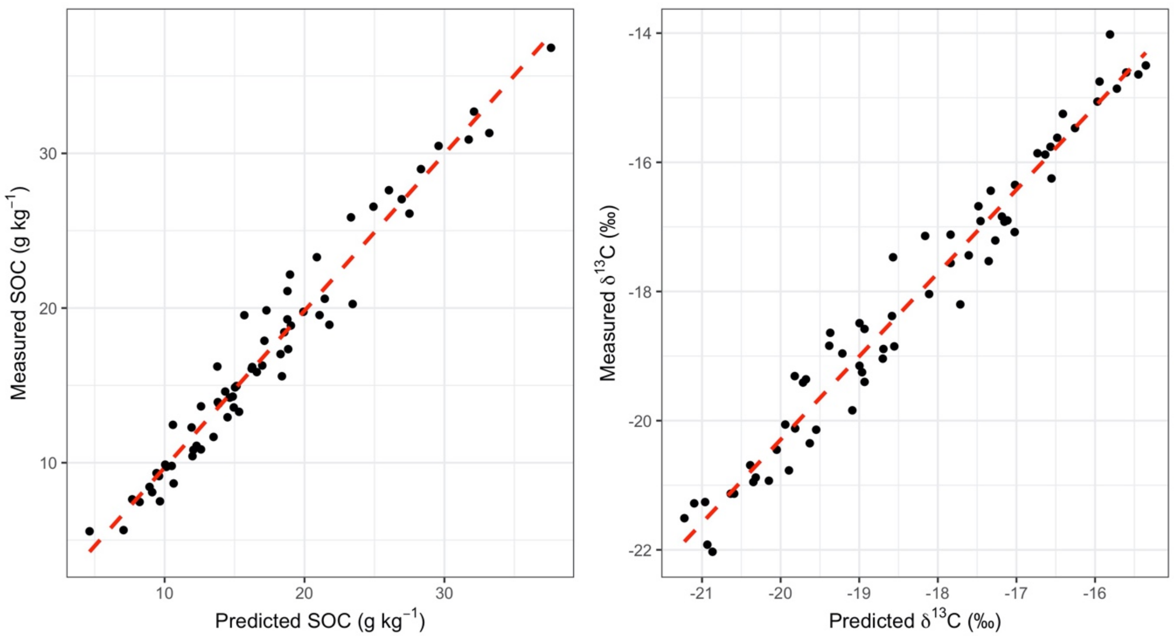

Figure 3. Predicted vs measured SOC and d13C based on MIR spectra for the two sites included in the study.

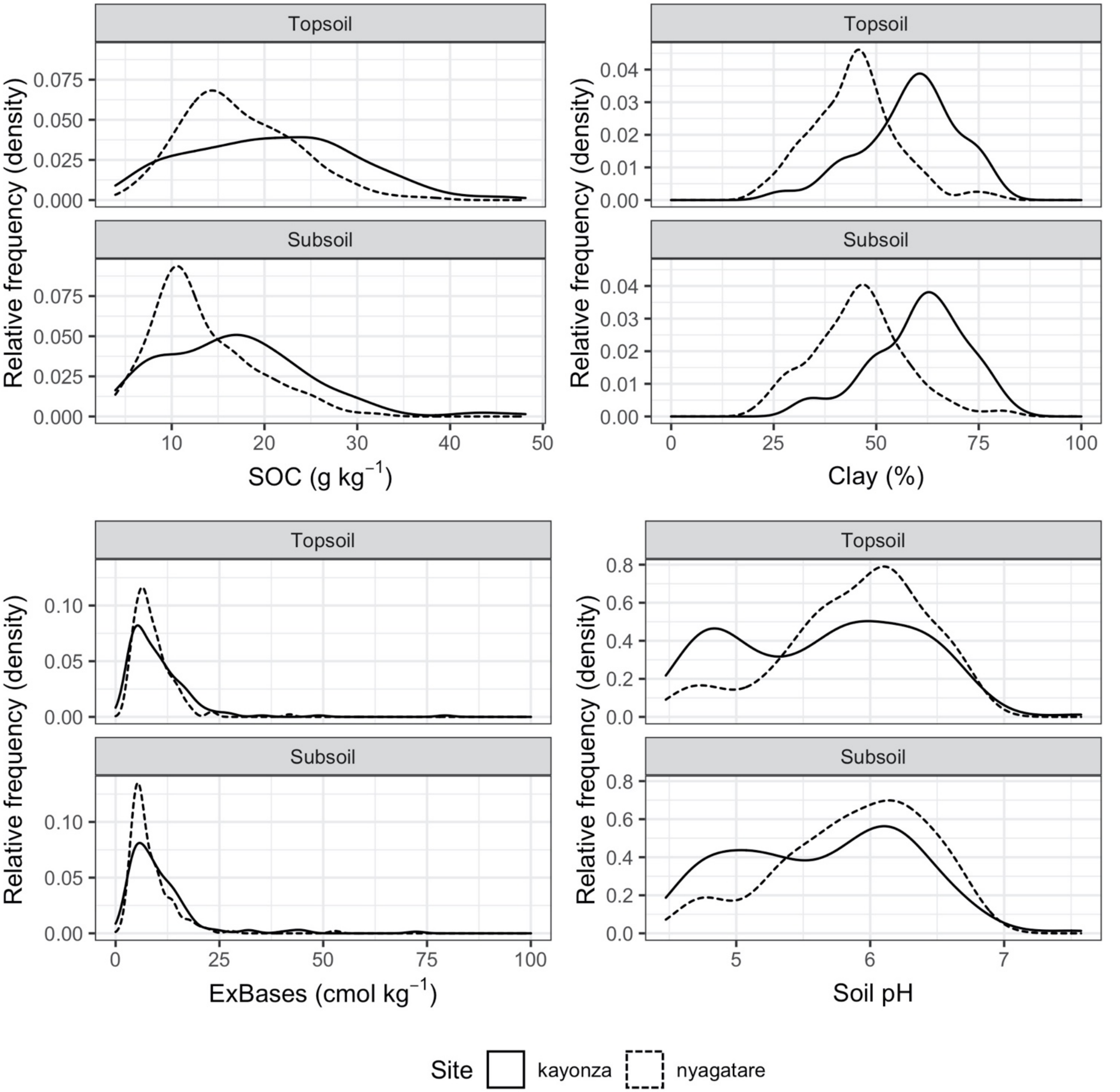

Figure 4: Density plots of soil organic carbon (SOC), clay, exchangeable bases (ExBases), and pH for the top and sub soil samples at Kayonza and Nygatare.

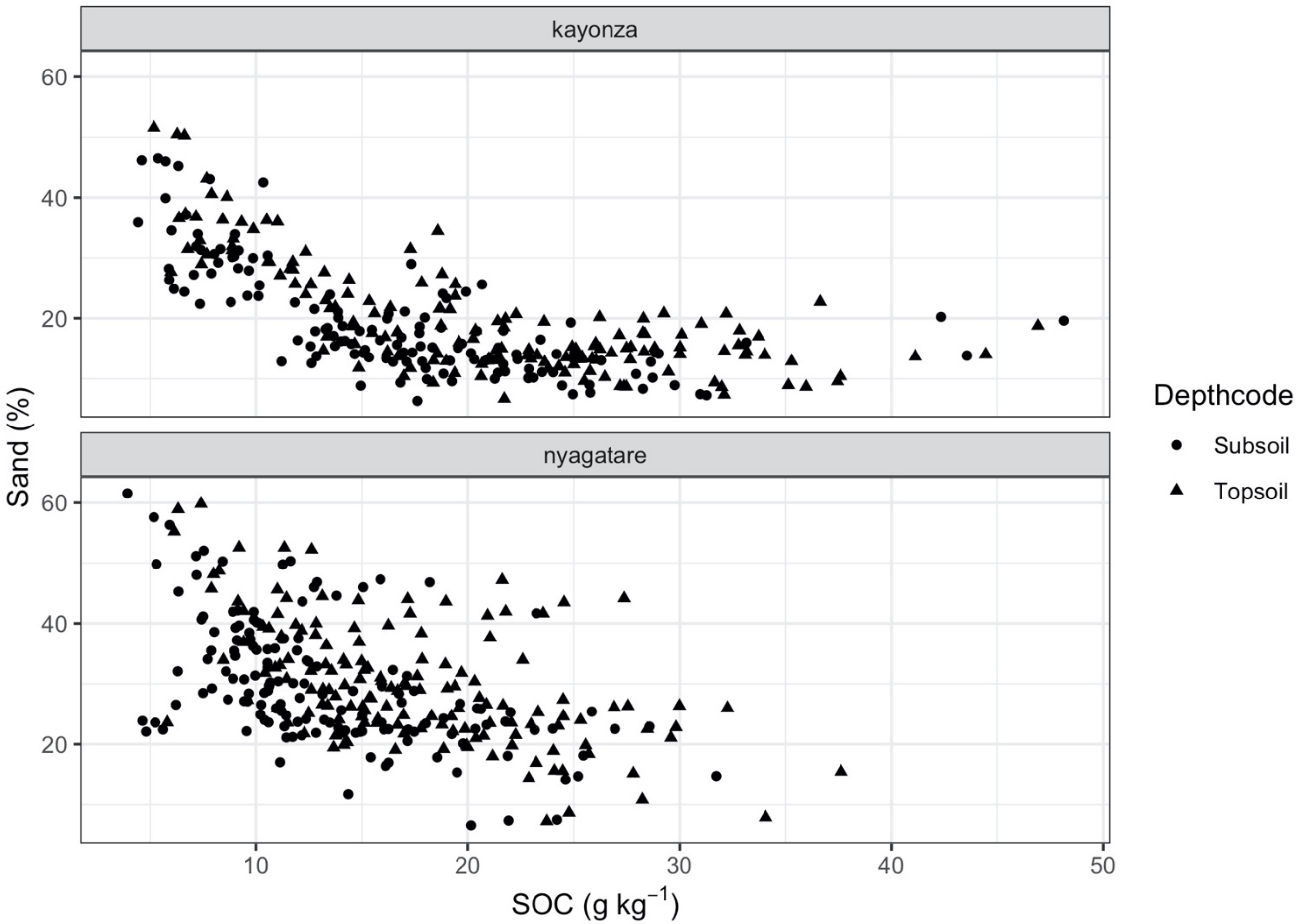

Figure 5: Relationship between sand content and soil organic carbon (SOC) for both top and sub soil samples at Kayonza nnd Nyagatare LDSF sites.

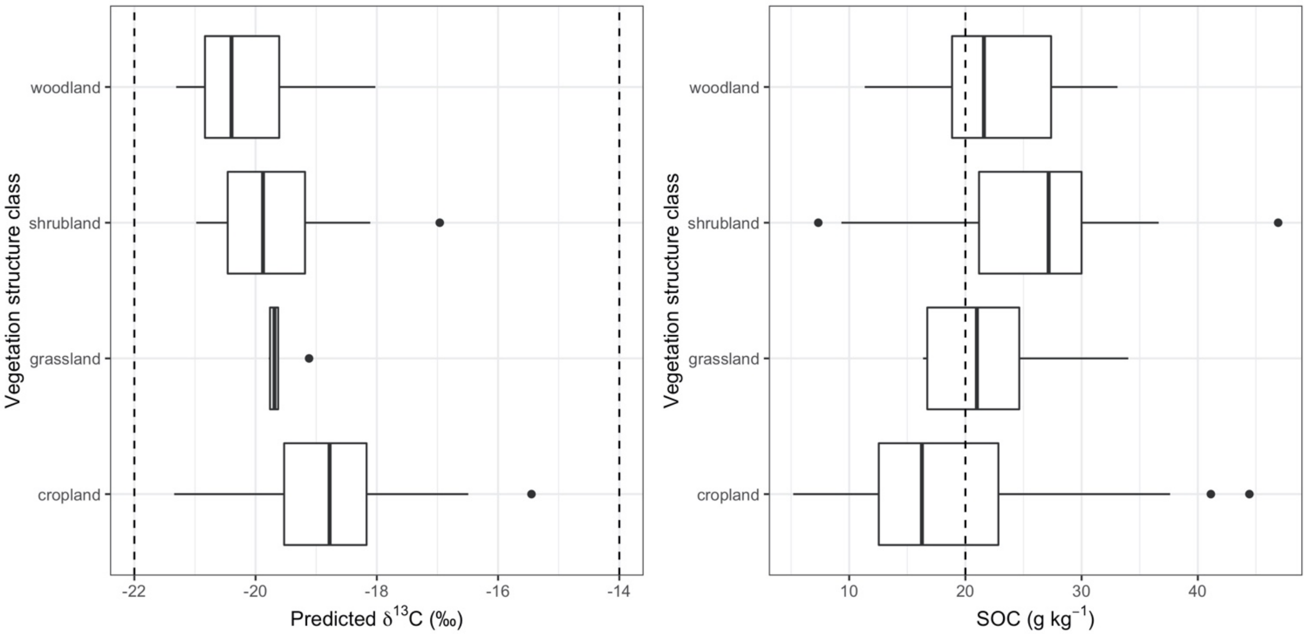

Figure 6: Boxplots of d13C values and SOC content in topsoil for each vegetation structure class. Dotted vertical lines at -22 and -14 ‰ indicate the C3 and C4 dominated systems, respectively. The dotted line at 20 g kg^{-1} SOC is to indicate a threshold for agricultural productivity in humid areas.

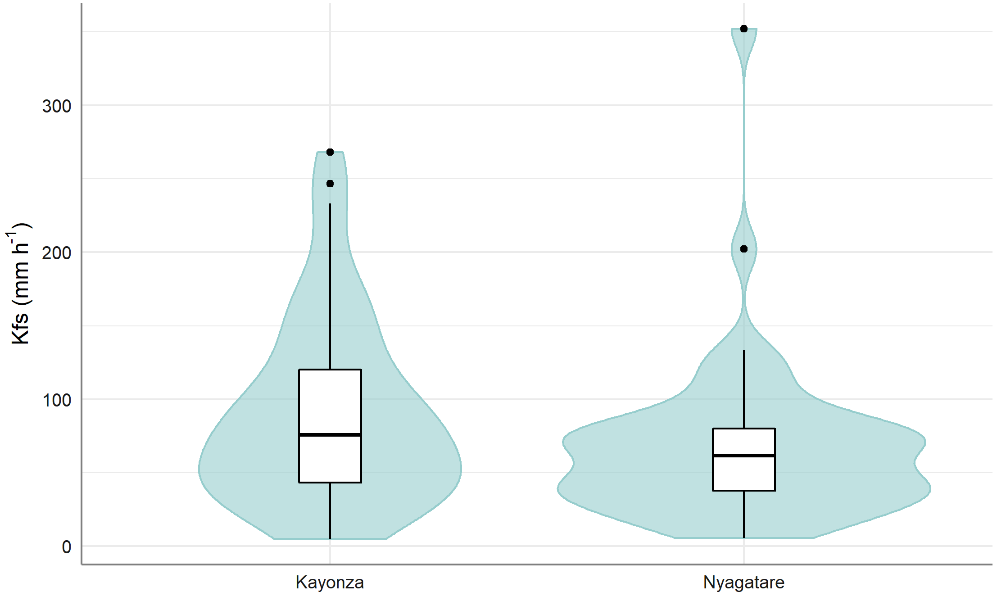

Figure 7: Box and violin plots of field-saturated hydraulic conductivity (Kfs) for each LDSF site. The three horizontal lines in the box plot show the lower quartile, the median, and the upper quartile. Whiskers extend to the outer-most data point that falls within 1.5 box lengths. The violin plots show the distribution of the Kfs data.

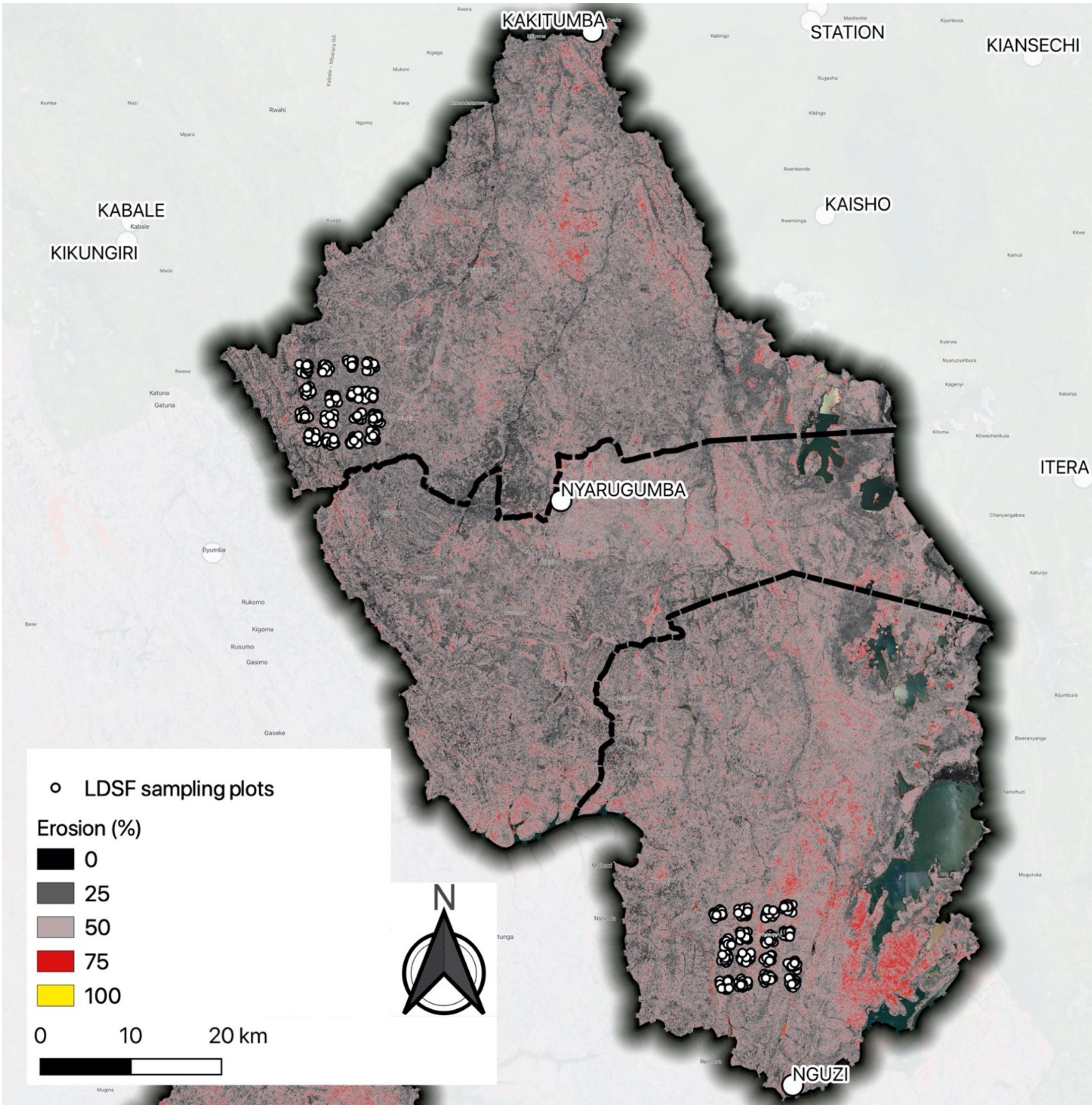

Figure 8: Map of soil erosion prevalence (%) predicted based on Landsat 8 satellite imagery and field data from the LDSF plots. The two LDSF sites are also shown on map (Nyagatare in the north and Kayonza in the south), with the sampling plots shown as white circles..

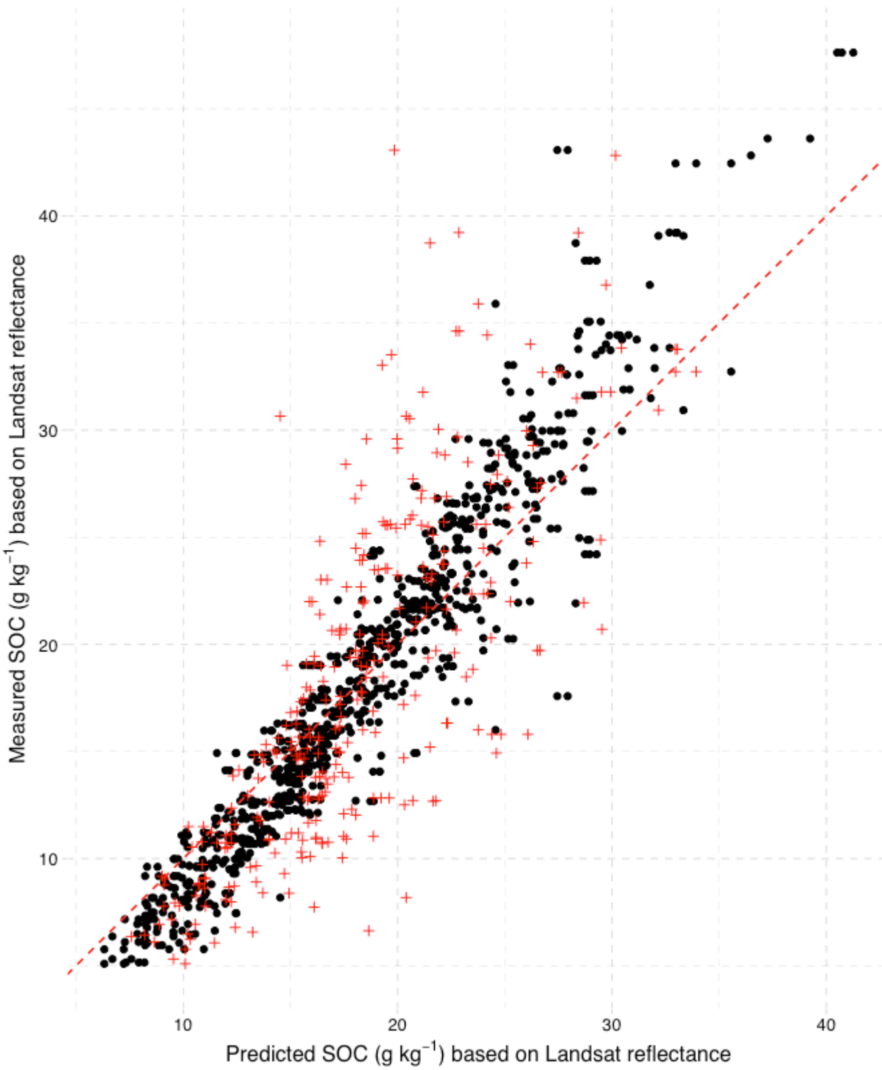

Figure 9. Predicted vs measured SOC based on predictions made from Landsat 8 reflectance for the two study sites. The black dots are training data, while the red crosses show independent validation results.

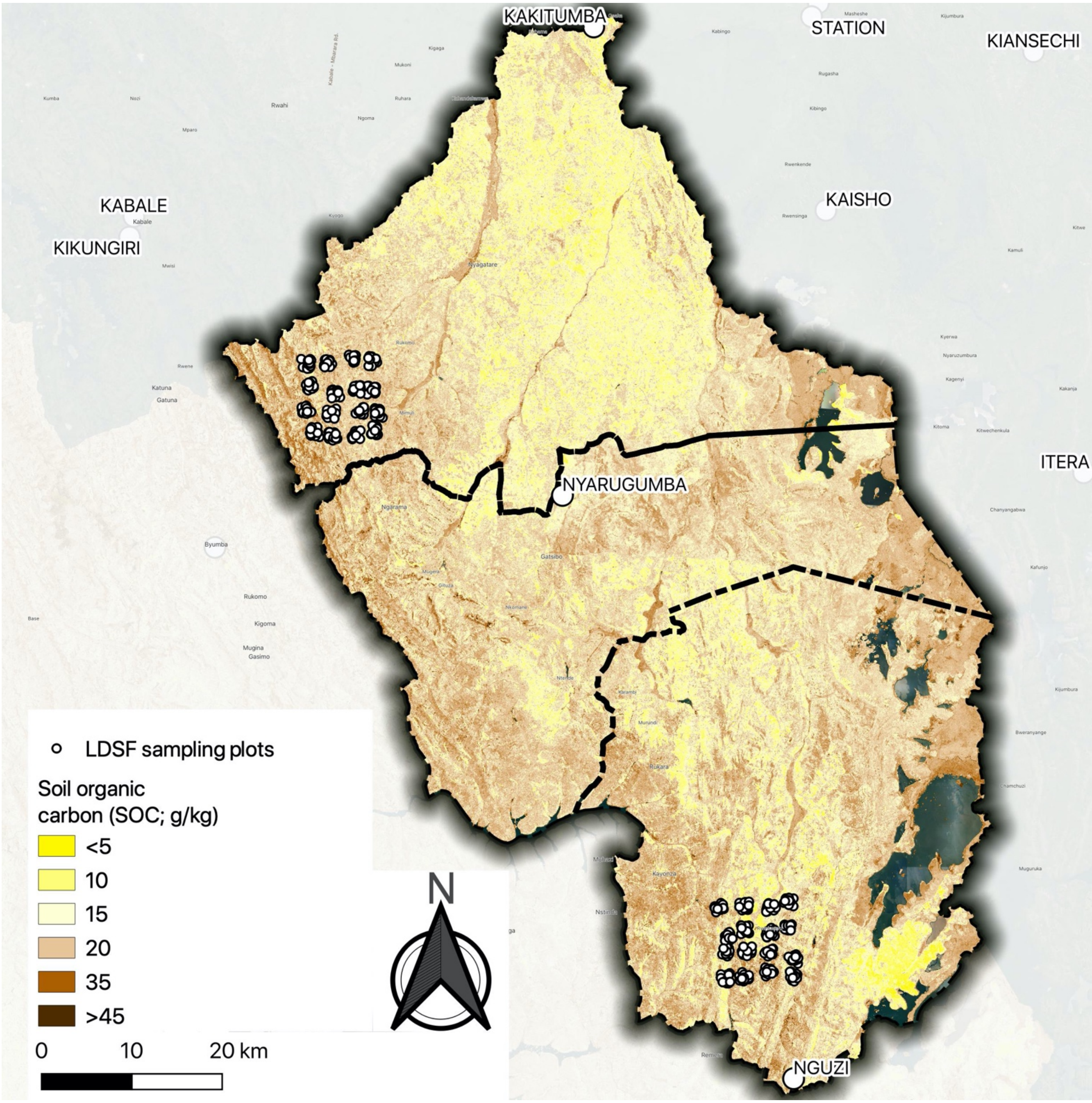

Figure 10. Map of soil organic carbon (SOC) predicted based on Landsat 8 satellite imagery and soil data from the LDSF plots. The two sites are also shown on map (Nyagatare in the north and Kayonza in the south), with the sampling plots shown as white circles.